Inorganic Chemistry

pubs.acs.org/IC Article

One-Dimensional Double Chains in Sodium-Based Quaternary Chalcogenides Displaying Intriguing Red Emission and Large Optical Anisotropy

Ya Yang, Kui Wu,* Bingbing Zhang,* Xiaowen Wu, and Ming-Hsien Lee



Cite This: Inorg. Chem. 2020, 59, 2519-2526



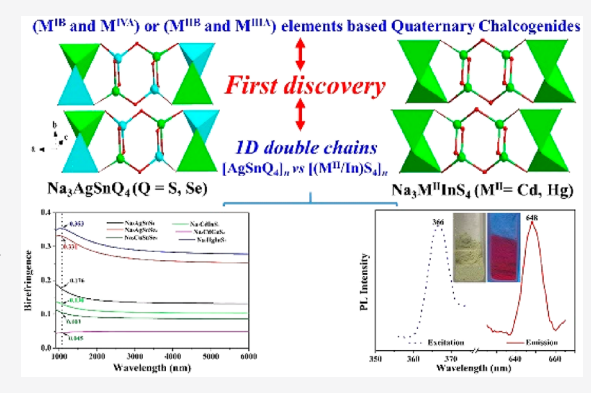
ACCESS

III Metrics & More

Article Recommendations

S Supporting Information

ABSTRACT: A new family of Na₃AgSnQ₄ (Q = S or Se) and Na₃M^{II}InS₄ (M^{II} = Cd or Hg) was successfully synthesized in vacuum-sealed silica tubes for the first time. They exhibit similar isolated one-dimensional (1D) double chains {[AgSnQ₄]_n vs [(M^{II}/In)S₄]_n} in their structures. After the detailed survey on the Inorganic Crystal Structure Database, title compounds can be described as the first discovered examples exhibiting novel 1D double-chain configurations in the known 171 (M^{IB} and M^{IVA}) or 48 (M^{IIB} and M^{IIIA}) element-based quaternary A-M^{IB}/M^{IIB}-M^{IVA}/M^{IIIA}-Q chalcogenides. In addition, their dimensionalities on the mode of connection between two anionic groups are closely related to the empirical A/(IB+IVA) and A/(IIB+IIIA) in the unit cell or the (IB+IVA)/Q and (IIB+IIIA)/Q ratios, which may produce a good way to predict and design new chalcogenides with low-dimensional structures. Photoluminescence measurement shows that Na₃CdGaS₄ and Na₃CdInS₄ display strong red



emission (648 and 647 nm) at room temperature that also agrees well with the change in color from yellow to red under the irradiation of an ultraviolet lamp. Moreover, all of the title crystals exhibit a large optical anisotropy ($\Delta n@1064$ nm ≥ 0.13), and isolated 1D double chains may produce a huge effect to enhance optical anisotropy based on the first-principles calculations, which also gives us a feasible way to design new birefringent materials.

■ INTRODUCTION

Chalcogenides, exhibiting multiple structural types and special physicochemical properties, have received a growing amount of attention and shown promise as critical candidates in many fields, such as laser technology, ¹⁻⁷ photoluminescence, ⁸⁻¹¹ photovoltaic, ¹²⁻¹⁵ thermoelectricity, ¹⁶⁻¹⁸ photocatalysis, ¹⁹⁻²¹ lithium or sodium batteries, etc. ²²⁻²⁶ Tetrahedral ligands are the most common basic building units in the metal chalcogenides and often form the larger dimeric or polymeric anionic groups by condensing. As we know, in general, common metal centers in the tetrahedral units are monovalent IB cations (M^{IB} = Ag or Cu), divalent IIB cations (M^{IIB} = Zn, Cd, or Hg), trivalent IIIA cations (MIIIA = Al, Ga, or In), and tetravalent IVA cations (M^{IVA} = Si, Ge, or Sn).²⁷⁻³⁰ In addition, the anionic groups mentioned above can also link together or bridge other cations to form extended structural motifs such as an isolated zero-dimensional (0D) unit, a onedimensional (1D) chain, a two-dimensional (2D) layer, and a three-dimensional (3D) network.31-33 Note that the substitution of the same main-group elements in the crystal structure can likely induce structural evolution because of the cation size effect, which has been discovered in many known chalcogenide systems. More importantly, alkali metals have been considered as the important reactants to be used to

improve the reaction environment and further increase the probability of new products; for example, Na atoms have variable coordination environments (NaQ_n, where n = 4-6) with a chalcogen (Q = S or Se), and NaQ_n ligands easily link with other anionic groups to form the novel structural features.^{34–36} On the basis of the analysis described above, it is feasible to design new compounds with novel structures by the interconnection of Na atoms and two different tetrahedral anionic groups, such as $M^{IB}Q_4$ and $M^{IVA}Q_4$ or $M^{IIB}Q_4$ and M^{IIIA}Q₄. In this work, we have chosen Na-(M^{IB} or M^{IIB})-(MIIIA or MIVA)-Q as the research system and four new quaternary compounds, Na₃AgSnQ₄ and Na₃M^{II}InS₄ (M^{II} = Cd or Hg), were successfully synthesized for the first time. They crystallize in different space groups: Na_3AgSnQ_4 ($P2_1/c$) versus Na₃M^{II}InS₄ (C2/m). Meanwhile, microcrystals of $Na_3CuSnSe_4$ and Na_3CdGaS_4 were also prepared for the structural and performance comparisons. Note that title crystals exhibit novel 1D double chains composed of

Received: November 24, 2019 Published: January 30, 2020



Table 1. Crystal Data and Structural Refinement for Title Compounds

empirical formula	Na ₃ AgSnSe ₄	Na ₃ AgSnS ₄	Na ₃ CuSnSe ₄	Na ₃ CdInS ₄	Na ₃ HgInS ₄	Na ₃ CdGaS ₄
formula weight	611.37	423.77	567.04	424.43	512.62	379.33
crystal system	monoclinic	monoclinic	monoclinic	monoclinic	monoclinic	tetragonal
space group	$P2_1/c$	$P2_1/c$	$P2_1/n$	C2/m	C2/m	I4 ₁ /acd
a (Å)	8.534(7)	8.109(4)	6.8083(16)	15.655(4)	15.675(4)	13.177(8)
b (Å)	6.758(6)	6.483(3)	10.233(2)	4.0453(12)	4.0542(9)	13.177(8)
c (Å)	16.574(14)	15.941(8)	13.033(3)	6.5507(19)	6.5478(15)	18.85(2)
β (deg)	104.106(11)	103.713(9)	90.419(5)	90.472(3)	90.499(3)	
$Z, V(\mathring{A}^3)$	4927.1 (14)	4814.0 (7)	4908.0 (4)	2414.8 (2)	2416.09 (16)	163272 (5)
$D_{\rm c}~({\rm g/cm^3})$	4.380	3.458	4.148	3.398	4.092	3.080
$\mu \left(\mathrm{mm}^{-1} \right)$	20.562	6.558	21.180	6.405	22.258	6.971
goodness of fit on F^2	0.940	1.039	0.969	1.182	1.136	1.133
R_1 , $wR_2 \left[I > 2\sigma(I)\right]^a$	0.0382, 0.0756	0.0305, 0.0490	0.0306, 0.0512	0.0206, 0.0217	0.0327, 0.0347	0.0322, 0.0450
R_1 , wR_2 (all data)	0.0688, 0.0781	0.0675, 0.0727	0.0508, 0.0564	0.0568, 0.0578	0.0965, 0.0983	0.0688, 0.0805
largest difference peak, hole (e $\mbox{Å}^{-3}$)	1.141, -1.620	2.433, -0.728	1.004, -1.143	0.701, -0.735	1.877, -1.550	0.950, -0.935
${}^{a}R_{1} = F_{0} - F_{c}/F_{0}$, and $wR_{2} = \left[w(F_{0}^{2} - F_{c}^{2})^{2}/wF_{0}^{4}\right]^{1/2}$ for $F_{0}^{2} > 2\sigma(F_{0}^{2})$.						

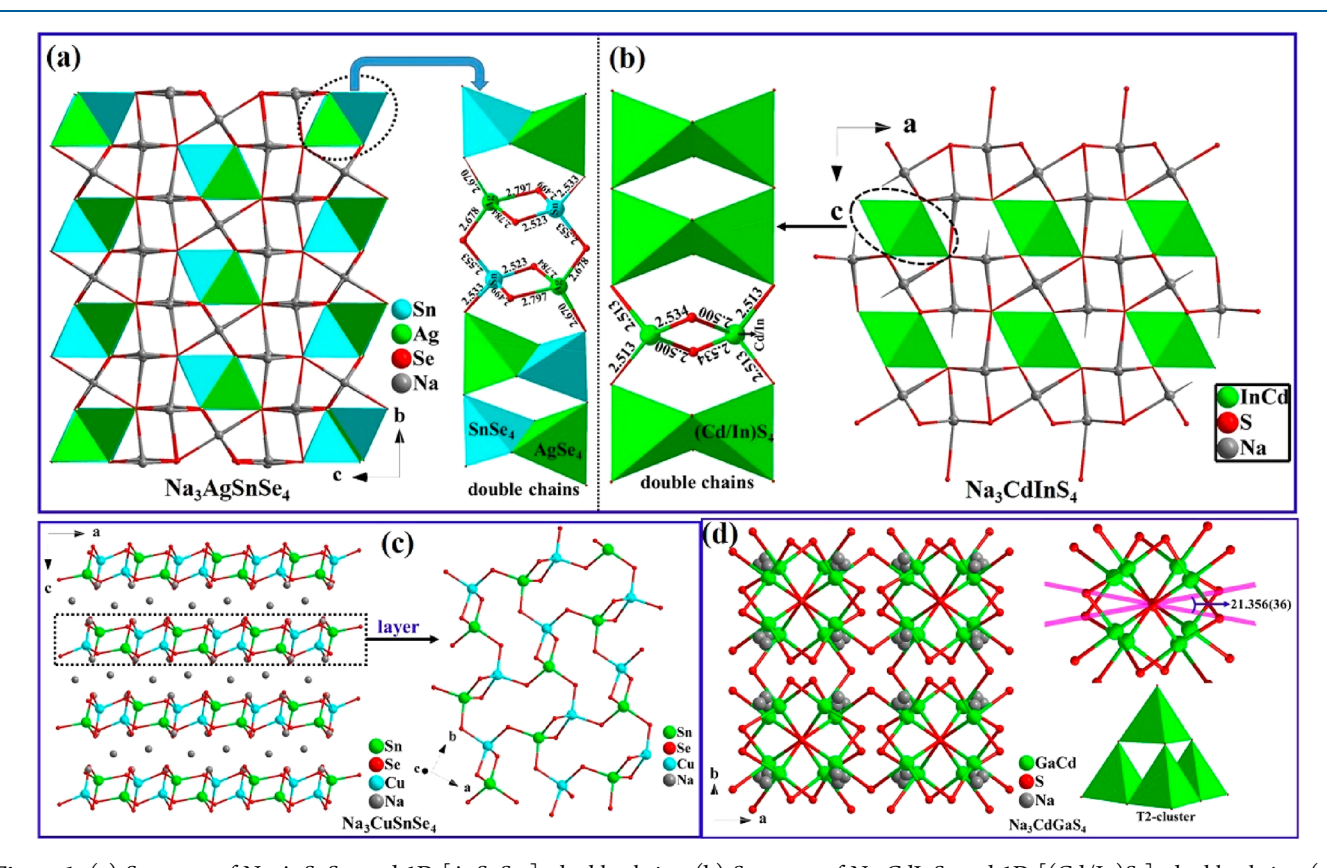


Figure 1. (a) Structure of $Na_3AgSnSe_4$ and 1D $[AgSnSe_4]_n$ double chains. (b) Structure of Na_3CdInS_4 and 1D $[(Cd/In)S_4]_n$ double chains. (c) Structure of $Na_3CuSnSe_4$ and the 2D layer. (d) Structure of Na_3CdGaS_4 and a T2 cluster with a torsion angle $[21.356(63)^{\circ}]$.

tetrahedral anionic groups, such as $[AgSnQ_4]_n$ double chains composed of AgQ_4 and SnQ_4 units in Na_3AgSnQ_4 and $[(M^{II}/In)S_4]_n$ chains composed of $(M^{II}/In)S_4$ units in $Na_3M^{II}InS_4$. After the detailed analysis of the Inorganic Crystal Structure Database (ICSD) data, one can note that the 1D double chains mentioned above are rarely found and title compounds can be viewed as the first discovered examples exhibiting the 1D double-chain configuration in the M^{IB} and M^{IVA} elements containing 171 quaternary chalcogenides or 48 M^{IIB} - and M^{IIIA} -based quaternary chalcogenides. Their band gap and photoluminescence performance were studied, and the results show that Na_3CdGaS_4 and Na_3CdInS_4 display the strong redemitting luminescence (\sim 648 nm) with excitation at 365 nm

as potential fluorescence materials. The structure–performance relationship was also systematically studied in terms of first-principles calculation, and all title crystals exhibit large optical anisotropy ($\Delta n@1064~\text{nm} \geq 0.13$) that may originate from the contribution of isolated 1D double chains in crystal structures.

■ RESULTS AND DISCUSSION

Title compounds crystallize in different space groups: Na_3AgSnQ_4 (Q = S or Se; $P2_1/c$) and $Na_3M^{II}InS_4$ (M^{II} = Cd or Hg; C2/m) (Table 1). We have chosen $Na_3AgSnSe_4$ and Na_3CdInS_4 as the representatives to depict their structures. As for $Na_3AgSnSe_4$, $AgSe_4$ ligands with d(Ag-Se) = 2.670-2.797

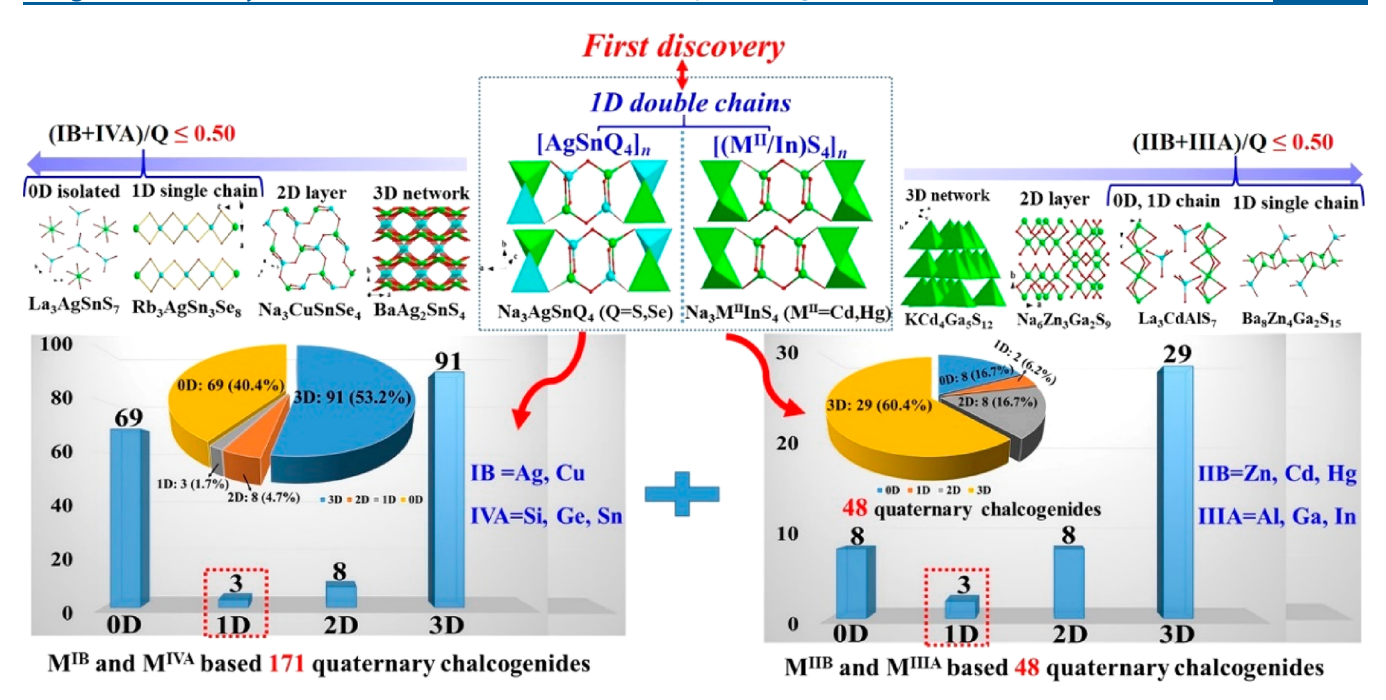


Figure 2. Summary of connection modes (from 0D to 3D) for anionic groups in 171 known IB- and IVA-based quaternary chalcogenides, including a histogram and a pie chart (left). Summary of connection modes (from 0D to 3D) for anionic groups in 48 known IIB- and IIIA-based quaternary chalcogenides, including a histogram and a pie chart (right).

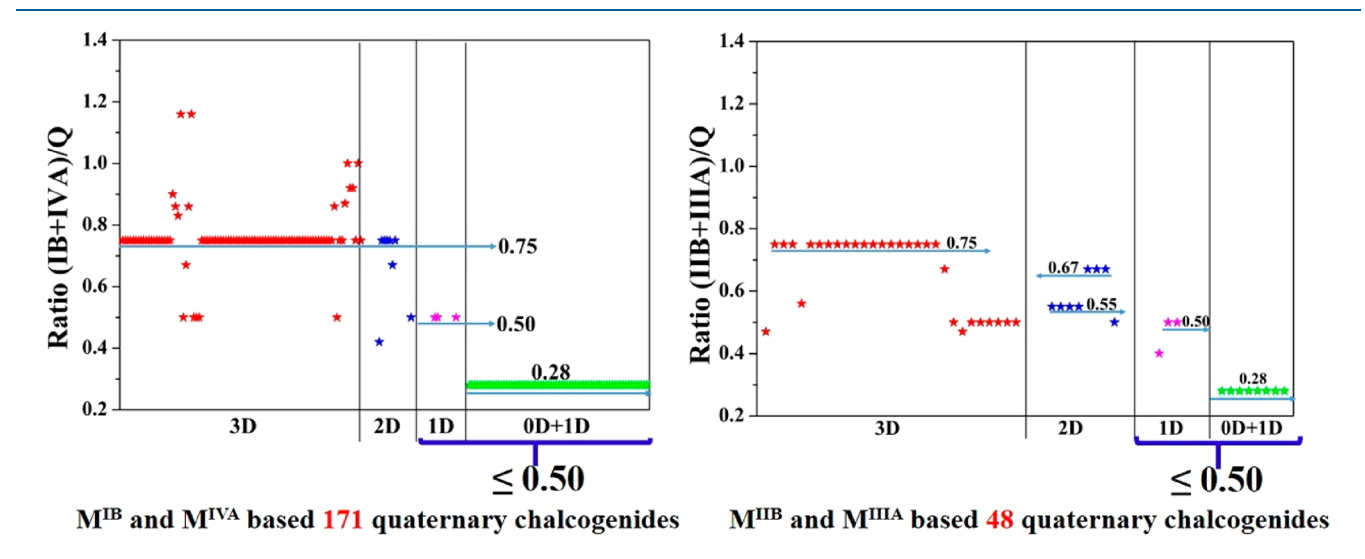


Figure 3. Schematic diagram of the empirical (IB+IVA)/Q ratio—structure relationships in 171 known IB- and IVA-based quaternary chalcogenides at a ratio of \leq 0.50 (tend to form the 1D or 0D type) (left). Schematic diagram of the empirical (IIB+IIIA)/Q ratio—structure relationships in 48 known IIB- and IIIA-based quaternary chalcogenides at a ratio of \leq 0.50 (tend to form the 1D or 0D type) (right).

Å and $SnSe_4$ units with d(Sn-Se) = 2.499-2.553 Å connect together to form the novel 1D $[AgSnSe_4]_n$ double chains (Figure 1a). $NaSe_6$ octahedra with d(Na-Se) = 2.830-3.516 Å link together to constitute the 3D tunnels within which the 1D chains are located. The connection mode described above (double chains) between $M^{IB}Q_4$ ($M^{IB} = Ag$ or Cu) and $M^{IVA}Q_4$ ($M^{IVA} = Si$, Ge, or Sn; Q = S or Se) units is rarely found in the known quaternary chalcogenides. After the survey of the Inorganic Crystal Structure Database (ICSD), it can be found that the modes of connection between $M^{IB}Q_4$ and $M^{IVA}Q_4$ in the known 171 quaternary chalcogenides have four structural configurations from 0D to 3D (Figure 2 and Table S3). Among them, 0D (69) and 3D (91) types exhibit maximum ratios of \sim 40.4% and \sim 53.2%, respectively. The

ratios of the 2D layer (8) and 1D chains (3) are 4.7% and 1.7%, respectively, for instance, Na₃CuSnSe₄ (2D layer) that formed by the interconnection of CuSe₄ and SnSe₄ units, which is different with the 1D double chains in Na₃AgSnSe₄ (Figure 1c). Similar structural changes with the substitution of Ag to Cu were also found: BaAg₂SnS₄ (1222) versus BaCu₂SnS₄ (P3₂2₁), ³⁷⁻³⁹ BaAg₂GeS₄ (142m) versus BaCu₂GeS₄ (P3₁2₁), ^{40,41} and Ag₈GeS₆ (Pna2₁)¹³ versus Cu₈GeS₆ (Pmn2₁). ^{42,43} Note that 1D chains have two different types: single and double chains. As for Rb₃AgSn₃Se₈, ⁴⁴ AgSe₄ and SnSe₄ units connect together by sharing edges to form the isolated 1D single chains whereas double chains in Na₃AgSnQ₄ are the first discovered structural feature in the known M^{1B} and M^{IVA}-based quaternary chalcogenides. As for Na₃CdInS₄, its

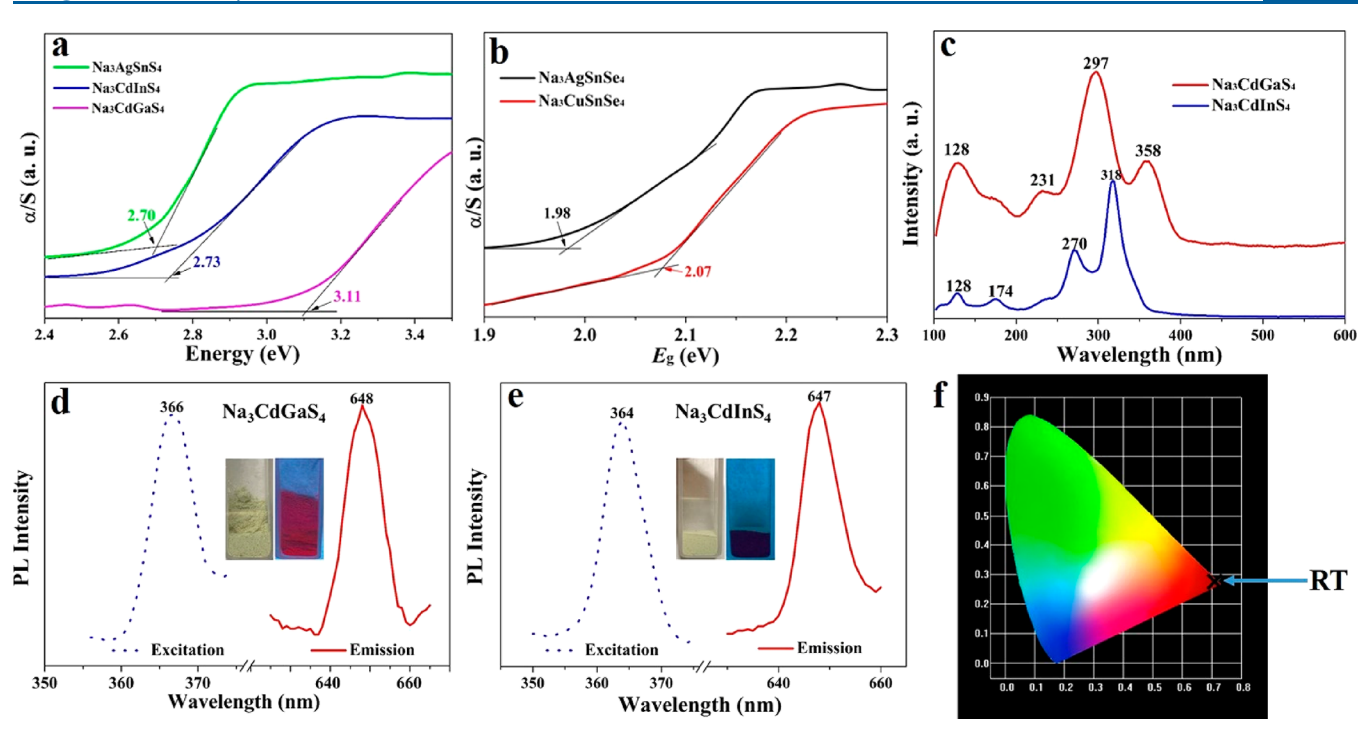


Figure 4. (a and b) Experimental band gaps. (c) Raman spectra of Na_3CdGaS_4 and Na_3CdInS_4 . (d and e) Photoluminescence of Na_3CdGaS_4 and Na_3CdInS_4 . The inset photos show the change in color under UV lamp irradiation. (f) Red fluorescence in the CIE-1931 diagram (RT = room temperature).

asymmetric unit is composed of two Na atoms, a 0.5:0.5 Cd:In ratio, and two S atoms. Note that $(Cd/In)S_4$ units with $d(Cd/In)S_4$ In-S) = 2.500–2.534 Å connect together by sharing corners and edges to form the 1D double [(Cd/In)S₄]_n chains (Figure 1b). Note that they undergo interesting structural changes after Ga is replaced with In atoms: Na₃CdInS₄ (C2/m) versus Na₃CdGaS₄ (I4₁/acd). Four (Cd/Ga)S₄ units link together by sharing corners to compose the typical T2 clusters, and adjacent T2 clusters exhibit a torsion angle of 21.356(36)° (Figure 1d). To analyze the structural characteristics, we have also studied the structures of known MIIB and MIIIA-based 48 quaternary chalcogenides and the result shows three types of connection modes in the system described above. Note that the 3D type occupies a major proportion of ~60.4% and the 2D layer or 0D types are $\sim 16.7\%$ (Table S5). So far, there are still no 1D double chains reported in the MIIB- and MIIIA-based chalcogenide system mentioned above (Figure 2). Thus, Na₃M^{II}InS₄ (M^{II} = Cd or Hg) can be considered as the first discovered examples exhibiting 1D double chains among the quaternary chalcogenides described above. Remarkably, detailed structural analysis also showed that their structural dimensionality is closely related to the change in the material formula, and the empirical (IB+IVA)/Q and (IIB+IIIA)/Q ratio can be used to judge the modes of connection of anionic groups in this work (Figure 2 and Tables S3 and S4). As for IB- and IVA-based quaternary chalcogenides, most of them are prone to forming 3D and 2D structure while (IB+IVA)/Q ≥ 0.75, and along with a decrease in the ratio (\leq 0.50), they are prone to forming the low-dimensional structure (1D and 0D). In addition, as for IIB- and IIIA-based systems, while the (IIB +IIIA)/Q ratio is ≥ 0.55 , most of them are more inclined to form the 3D and 2D structures whereas they form the 1D or 0D structures with a ratio of \leq 0.50. Thus, an empirical ratio of 0.5 may be viewed as the turning point for the structural changes described above (Figure 3). Moreover, to prove the

structural novelty of 1D double chains, we have calculated the A/(IB+IVA) or A/(IIB+IIIA) number ratios in the unit cell and the result shows that the formation of the 1D double chain requires a ratio of 2.0. While the ratio is <1.0, all of them exhibit a 3D network. Along with the increase in the ratio, they are inclined to form the 2D layer structure. However, for the A-IIB-IIIA-Q system, it is partially similar to that in the A-IB-IVA-Q system; some still exhibit exceptions. Although several of them exhibit a ratio of 2.0, their anionic groups are prone to forming the 3D network because of their small tetrahedral sizes compared to those of Na₃M^{IIB}InS₄. Small tetrahedral units are unstable in the tunnels formed by the NaS₆ ligands that have to connect together to possess the 3D network. On the basis of the analysis described above, their dimensionalities on the connection modes between two anionic groups have a close relationship with the empirical A/(IB+IVA) and A/(IIB+IIIA) ratios in the unit cell or (IB +IVA)/Q and (IIB+IIIA)/Q ratios, and note that the form of low-dimensional (1D and 0D) structural features should satisfy the following conditions: (1) A/(IB+IVA) and (IIB+IIIA) ratios of ≥2.0, such as Na₃AgSnQ₄ (2.0) and Na₃M^{II}InS₄ (2.0); (2) (IB+IVA)/Q and (IIB+IIIA)/Q ratios of ≤ 0.50 , such as Na₃AgSnQ₄ (0.5) and Na₃M^{II}InS₄ (0.5); and (3) tetrahedral anionic groups that might as well be the large volumes or central metal cations with high molecular weights, such as IB = Cu and IIB = Zn with low molecular weights (there is no 1D double chain in their structures). In addition, other quaternary chalcogenides are not in accordance with the rule mentioned above; thus, 1D double chains have not been observed in the other quaternary chalcogenides. Therefore, title crystals are the first discovered examples with novel 1D double chains in the 219 known quaternary compounds.

High-quality title crystals were obtained by the high-temperature solid-state method in vacuum-sealed silica tubes. Their polycrystalline samples were prepared with a stoichio-

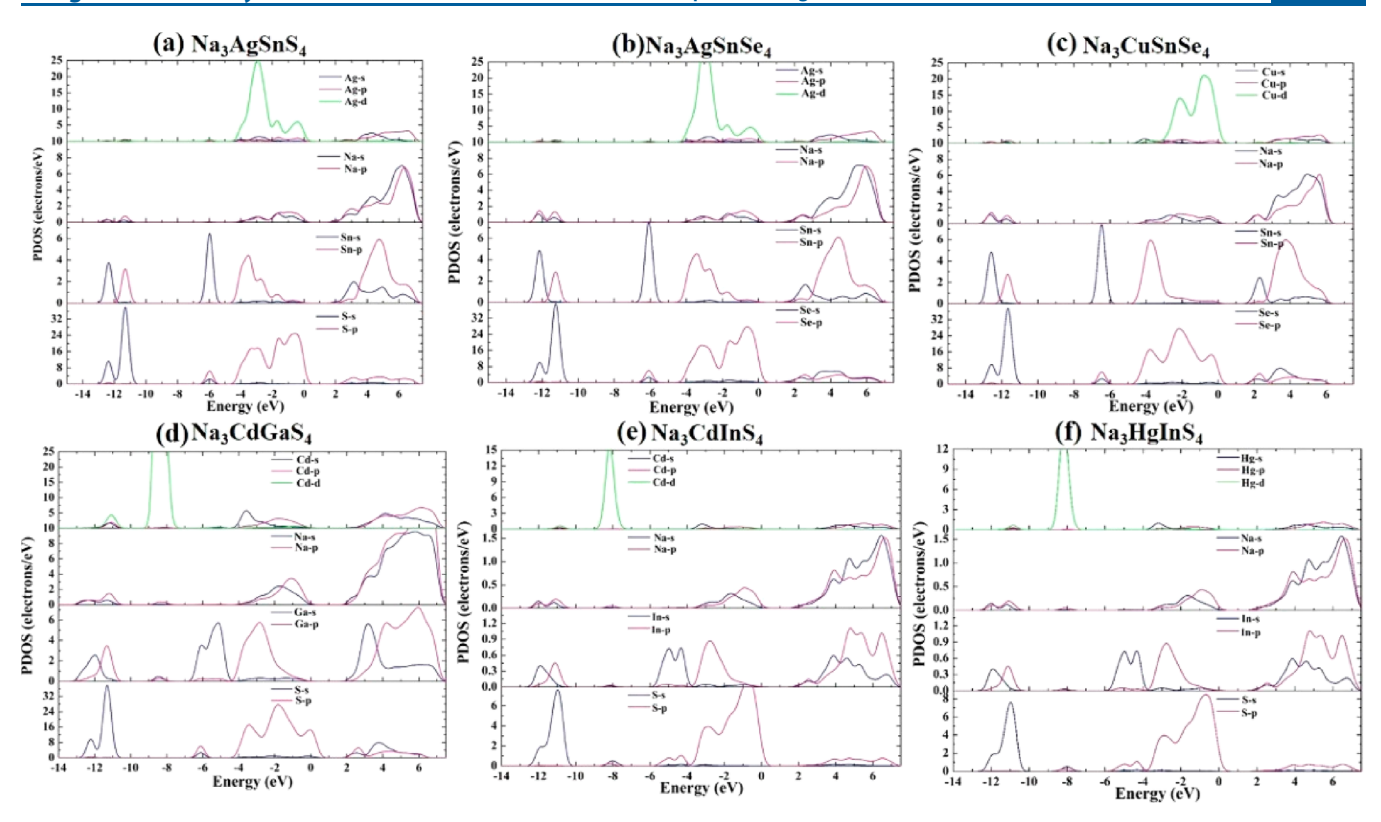


Figure 5. Partial densities of states (PDOS) of title compounds.

metric ratio except for Na₃HgInS₄, which was not successfully achieved at the different ratios or reaction temperatures. Among them, Na₃M^ISnQ₄ samples show obvious moisture absorption with a change in crystal surface color from red to black in the air within a split second and Na₃M^{II}InS₄ samples are relatively stable in air over several days. This phenomenon has a close relationship with their 3D network structures composed of interconnection of NaQ₆ octahedra that are completely exposed to the air.⁴⁵ Thus, we have measured the experimental powder XRD patterns in the vacuum apparatus, which are in agreement with theoretical ones, and the intensity differences can be attributed to the preferred orientation (Figure S2). Herein, we have also studied their physicochemical performances (band gap, Raman spectra, and photoluminescence) (Figure 4). Their band gaps are 1.98 eV for Na₃AgSnSe₄, 2.07 eV for Na₃CuSnSe₄, 2.70 eV for Na₃AgSnS₄, 2.73 eV for Na₃CdInS₄, and 3.11 eV for Na₃CdGaS₄ (Figure 4a,b). Along with the element substitution in the same main groups, their band gaps undergo an obvious decrease with an increase in molecular weight (from Cu to Ag, Ga to In, or S to Se). Considering the air-sensitive title compounds, we have measured the Raman luminescence and photoluminescence of only Na₃CdInS₄ and Na₃CdGaS₄. As for the Raman spectra, it can be seen that the strongest peaks are located at 297 and 318 nm for Na₃CdInS₄ and Na₃CdGaS₄, respectively (Figure 4c). In addition, the peaks located between 200 and 300 nm, such as 231, 297, and 358 nm for Na₃CdGaS₄ and 270 and 318 nm for Na₃CdInS₄, can be attributed to the vibration of (Cd/Ga)-S and (Cd/In)-S bonds, respectively, which are also similar to these reported results in related compounds. 46-48 Several peaks (128 and 174 nm) below 200 nm can also be attributed to the Na-S bond vibration. Moreover, at excitation wavelengths of approximately 364-366 nm, Na₃CdGaS₄ and Na₃CdInS₄ display a strong emission band centered at 648 or 647 nm at room temperature (RT), which indicate the interesting red-emitting luminescence. We have also used the ultraviolet (UV) lamp to verify the photoluminescence phenomenon, and the sample shows the obvious change in color from yellow to red, which also shows the reliability of the PL test results (Figure 4d,e). The photoluminescence quantum vields are 1.24% and 1.53% for Na₃CdGaS₄ and Na₃CdInS₄, respectively, at room temperature, and their fluorescence lifetimes are 9.6 and 13.4 μ s, respectyively, at room temperature (Figure S3). In comparison with related $ACd_4Ga_5S_{12}$ (A = K, Rb, or Cs) compounds, 8 title compounds show similar quantum yields but shorter fluorescence lifetimes. We can fine no explicit reason for this change in fluorescence lifetimes between title compounds and ACd₄Ga₅S₁₂ compounds, but ACd₄Ga₅S₁₂ compounds have more disorder locations (three Cd/Ga) than one Cd/M^{III} in title compounds that induces the change in fluorescence lifetimes mentioned above. In comparison with these reported chalcogenides, several of them show similar fluorescence emission, for example, $ACd_4Ga_5S_{12}$ (A = K, Rb, or Cs) (yellow, 584–595 nm),⁸ Ba₆Zn₇Ga₂S₁₆ (yellow, 600 nm),¹⁰ Rb₂Au₂Cd₂S₄ (red, 624 nm), 49 Ba₈Zn₄Ga₂S₁₅ (yellow, 593 nm), 11 K₂Cd₃S₄ (red, 646 nm), 50 BaCdSnS₄ (yellow, 530 nm), and Ba₃CdSn₂S₈ (yellow, 530 nm). 51 A summary of the fluorescence emission performance of these materials is shown in Table S5. Analysis of the reported results can indicate that all of them show obvious fluorescence emission in the yellow to red region, and the emission transition mentioned above may originate from the electron transition in various defects or disordered structure. Therefore, we think that the materials described above have promising potential as excellent hosts for the introduction of the various photoluminescent centers to achieve multiple emission outputs.

To better investigate the structure—performance relationship of title compounds, we have also calculated their electronic structures on the basis of the first-principles calculation. Their theoretical band gaps are 1.66 for Na₃AgSnS₄, 1.26 for Na₃AgSnSe₄, 1.28 for Na₃CuSnSe₄, 1.83 for Na₃CdGaS₄, 1.77 for Na₃CdInS₄, and 1.34 eV for Na₃HgInS₄ (Figure S4). All of them are lower than the experimental values, which are usually underestimated by GGA calculations. 52 Their partial densities of states (PDOS) were also studied, and Na₃AgSnS₄ and Na₃CdInS₄ were chosen as the representatives (Figure 5). As for Na₃AgSnS₄, obvious hybridization of Sn 5s and 5p, Ag 4d. and S 3s orbitals between -15 and -5 eV corresponds to the Sn-S and Ag-S bonds. Also, for the upper part of the valence bond [VB, -5 eV to Fermi level (FL)], a few hybridizations exist among Sn 5p, S 3p, and Ag 4d and 5s orbitals. In addition, the bottom of the conduction bond (CB) is mainly composed of S 3p, Sn 5s and 5p, and Ag 5s states. Thus, the AgS₄ and SnS₄ units determine the optical band gap of Na₃AgSnS₄, which can also extend to the effect on the optical absorption of Na₃AgSnSe₄ (AgSe₄ and SnSe₄) and Na₃CuSnSe₄ (CuSe₄ and SnSe₄). In addition, as for Na₃CdInS₄, its VB region near the FL is dominated by Cd 5s and 5p and S 3p mixing with In 5s and 5p states. The region located at the bottom of the CB is derived primarily from the S 3p, In 5s and 5p, and Cd 5s and 5p states. Thus, the $(Cd/In)S_4$ units determine the optical band gap of Na₃CdInS₄, which can also extended to the optical absorption of other related title compounds (Na₃CdGaS₄ and Na₃HgInS₄). To study their optical anisotropy, we have calculated their refractive indices, and their birefringences at 1064 nm are 0.176 for Na₃AgSnS₄, 0.331 for Na₃AgSnSe₄, 0.103 for Na₃CuSnSe₄, 0.045 for Na₃CdGaS₄, 0.130 for Na₃CdInS₄, and 0.353 for Na₃HgInS₄ (Figure 6). Interestingly, we note that their birefringences

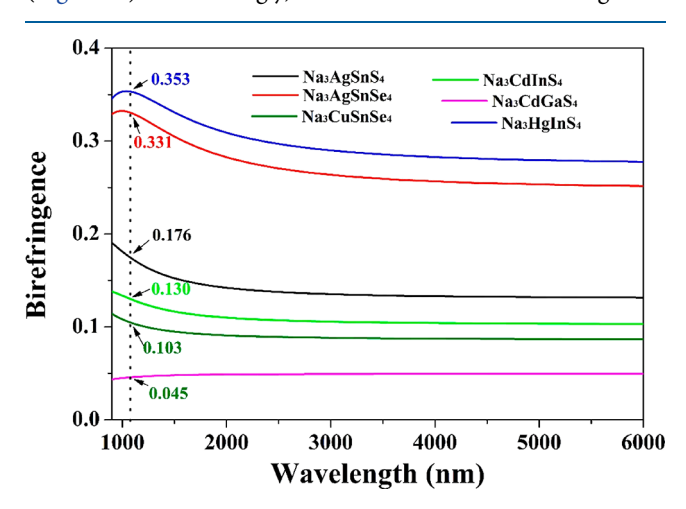


Figure 6. Birefringence of title compounds.

undergo obvious changes with the transformation of space groups upon substitution with different cations. Thus, the optical anisotropy of the material is closely related with its crystal structure; for instance, via comparison of the crystal structures of Na₃AgSnSe₄ and Na₃CuSnSe₄, they undergo the structural transformation from a 2D layer to 1D chains composed of tetrahedral anionic groups, and the birefringence shows an obvious decrease from 0.331 to 0.103, which is similar to those of Na₃CdInS₄ (1D chains, 0.130) and Na₃CdGaS₄ (3D network, 0.045). Moreover, we have also calculated the birefringence of 1D single chains containing

related quaternary chalcogenides, such as Ba₈Zn₄Ga₂S₁₅ (0.120@1064 nm) and Rb₃AgSn₃Se₈ (0.335@1064 nm). Other 0D and 1D single chain-based quaternary chalcogenides crystallize in the *P*6₃ space group, and their birefringences have been not studied; however, several isostructural compounds have been reported, such as La₃Ge_{0.5}GaS₇ (0.023), La₃Ge_{0.5}InS₇ (0.007), and Sm₃In_{0.33}GeS₇ (0.008). One can conclude that isolated 1D double chains may produce a huge effect to enhance the optical anisotropy, which also gives us a new method for designing new potential birefringent materials.

CONCLUSIONS

In summary, the crystal structures and physicochemical properties of new series of quaternary chalcogenides were systematically studied and characterized. Note that they exhibit novel 1D double chains that can be viewed as the first discovered structural configuration after a survey of the known M^{IB}- and M^{IVA}-based or M^{IIB}- and M^{IIIA}-based quaternary chalcogenides. A detailed investigation shows that Na₃CdGaS₄ and Na₃CdInS₄ display strong red emission and have promise as critical materials in the photoluminescence field. Moreover, title crystals also undergo an obvious change in optical anisotropy with cation substitution, which also gives us a feasible way to design new birefringent materials.

ASSOCIATED CONTENT

Solution Supporting Information

The Supporting Information is available free of charge at https://pubs.acs.org/doi/10.1021/acs.inorgchem.9b03444.

Experimental details, bond lengths, a summary of structural features, and powder XRD data (PDF)

Accession Codes

CCDC 1944976–1944981 contain the supplementary crystallographic data for this paper. These data can be obtained free of charge via www.ccdc.cam.ac.uk/data_request/cif, or by emailing data_request/cif, or by contacting The Cambridge Crystallographic Data Centre, 12 Union Road, Cambridge CB2 1EZ, UK; fax: +44 1223 336033.

AUTHOR INFORMATION

Corresponding Authors

Kui Wu — Key Laboratory of Medicinal Chemistry and Molecular Diagnosis of the Ministry of Education, Key Laboratory of Analytical Science and Technology of Hebei Province, College of Chemistry and Environmental Science, Hebei University, Baoding 071002, China; ⊚ orcid.org/0000-0001-8242-4613; Email: wukui@hbu.edu.cn

Bingbing Zhang — Key Laboratory of Medicinal Chemistry and Molecular Diagnosis of the Ministry of Education, Key Laboratory of Analytical Science and Technology of Hebei Province, College of Chemistry and Environmental Science, Hebei University, Baoding 071002, China; Email: zhangbing@hbu.edu.cn

Authors

Ya Yang — Key Laboratory of Medicinal Chemistry and Molecular Diagnosis of the Ministry of Education, Key Laboratory of Analytical Science and Technology of Hebei Province, College of Chemistry and Environmental Science, Hebei University, Baoding 071002, China

Xiaowen Wu – Key Laboratory of Medicinal Chemistry and Molecular Diagnosis of the Ministry of Education, Key

Laboratory of Analytical Science and Technology of Hebei Province, College of Chemistry and Environmental Science, Hebei University, Baoding 071002, China

Ming-Hsien Lee – Department of Physics, Tamkang University, New Taipei City 25137, Taiwan

Complete contact information is available at: https://pubs.acs.org/10.1021/acs.inorgchem.9b03444

Notes

The authors declare no competing financial interest.

ACKNOWLEDGMENTS

This work was supported by the National Natural Science Foundation of China (Grants 51872324, 21763026, and 51702356), the Natural Science Foundation of Hebei Province (Grants E2019201049 and B2019201433), and the Advanced Talents Incubation Program of Hebei University (801260201293).

REFERENCES

- (1) Li, S. F.; Jiang, X. M.; Fan, Y. H.; Liu, B. W.; Zeng, H. Y.; Guo, G. C. New strategy for designing promising mid-infrared nonlinear optical materials: narrowing the band gap for large nonlinear optical efficiencies and reducing the thermal effect for a high laser-induced damage threshold. *Chem. Sci.* **2018**, *9*, 5700–5708.
- (2) Chung, I.; Kanatzidis, M. G. Metal chalcogenides: a rich source of nonlinear optical materials. *Chem. Mater.* **2014**, *26*, 849–869.
- (3) Liang, F.; Kang, L.; Lin, Z. S.; Wu, Y. C. Mid-Infrared Nonlinear Optical Materials Based on Metal Chalcogenides: Structure-Property Relationship. *Cryst. Growth Des.* **2017**, *17*, 2254–2289.
- (4) Xing, X. S.; Sa, R. J.; Li, P. X.; Zhang, N. N.; Zhou, Z. Y.; Liu, B. W.; Liu, J.; Wang, M. S.; Guo, G. C. Second-order nonlinear optical switching with a record-high contrast for a photochromic and thermochromic bistable crystal. *Chem. Sci.* **2017**, *8*, 7751–7757.
- (5) Luo, Z. Z.; Lin, C. S.; Cui, H. H.; Zhang, W. L.; Zhang, H.; Chen, H.; He, Z. Z.; Cheng, W. D. PbGa₂MSe₆ (M = Si, Ge): Two Exceptional Infrared Nonlinear Optical Crystals. *Chem. Mater.* **2015**, 27, 914–922.
- (6) Li, M. Y.; Li, B. X.; Lin, H.; Shi, Y. F.; Ma, Z. J.; Wu, L. M.; Wu, X. T.; Zhu, Q. L. Ternary Mixed-Metal Cd₄GeS₆: Remarkable Nonlinear-Optical Properties Based on a Tetrahedral-Stacking Framework. *Inorg. Chem.* **2018**, *57*, 8730–8734.
- (7) Li, M. Y.; Li, B. X.; Lin, H.; Ma, Z. J.; Wu, L. M.; Wu, X. T.; Zhu, Q. L. Sn₂Ga₂S₅: A Polar Semiconductor with Exceptional Infrared Nonlinear Optical Properties Originating from the Combined Effect of Mixed Asymmetric Building Motifs. *Chem. Mater.* **2019**, *31*, 6268–6275.
- (8) Lin, H.; Zhou, L. J.; Chen, L. Sulfides with Strong Nonlinear Optical Activity and Thermochromism: $ACd_4Ga_5S_{12}(A = K, Rb, Cs)$. *Chem. Mater.* **2012**, *24*, 3406–3414.
- (9) Kim, C. D.; Jeong, H. M.; Kim, H. G.; Kim, W. T. Photoluminescence Spectra of CdGa₂Se₄ Single Crystals. *J. Korean Phys. Soc.* **1994**, 27, 440.
- (10) Li, Y. Y.; Liu, P. F.; Wu, L. M. Ba₆Zn₇Ga₂S₁₆: A Wide Band Gap Sulfide with Phase-Matchable Infrared NLO Properties. *Chem. Mater.* **2017**, 29, 5259–5266.
- (11) Li, Y. Y.; Liu, P. F.; Lin, H.; Wu, L. M.; Wu, X. T.; Zhu, Q. L. Quaternary semiconductor $Ba_8Zn_4Ga_2S_{15}$ featuring unique one-dimensional chains and exhibiting desirable yellow emission. *Chem. Commun.* **2019**, *55*, 7942–7945.
- (12) Chen, M. M.; Xue, H. G.; Guo, S. P. Multinary metal chalcogenides with tetrahedral structures for second-order nonlinear optical, photocatalytic, and photovoltaic applications. *Coord. Chem. Rev.* 2018, 368, 115–133.
- (13) Kishore Kumar, Y.B.; Suresh Babu, G.; Uday Bhaskar, P.; Sundara Raja, V. Preparation and characterization of spray-deposited

- Cu₂ZnSnS₄ thin films. Sol. Energy Mater. Sol. Cells 2009, 93, 1230–1237.
- (14) Guo, Q. J.; Hillhouse, H. W.; Agrawal, R. Synthesis of $\text{Cu}_2\text{ZnSnS}_4\text{Nanocrystal}$ Ink and Its Use for Solar Cells. *J. Am. Chem. Soc.* **2009**, *131*, 11672–11673.
- (15) Draguta, S.; McDaniel, H.; Klimov, V. I. Tuning Carrier Mobilities and Polarity of Charge Transport in Films of CuInSe_xS_{2-x} Quantum Dots. *Adv. Mater.* **2015**, 27, 1701–1705.
- (16) Kim, J. H.; Chung, D. Y.; Bilc, D.; Loo, S.; Short, J.; Mahanti, S. D.; Hogan, T.; Kanatzidis, M. G. Crystal Growth, Thermoelectric Properties, and Electronic Structure of $AgBi_3S_5$ and $AgSb_xBi_{3-x}S_5$ (x = 0.3). Chem. Mater. **2005**, 17, 3606–3614.
- (17) Rowe, D. M. CRC Handbook of Thermoelectric Materials; CRC Press: Boca Raton, FL, 1995.
- (18) Mrotzek, A.; Kanatzidis, M. G. Design" in Solid-State Chemistry Based on Phase Homologies. The Concept of Structural Evolution and the New Megaseries $A_m[M_{1+l}Se_{2+l}]_{2m}[M_{2l+n}Se_{2+3l+n}]$. Acc. Chem. Res. **2003**, 36, 111–119.
- (19) Tabata, M.; Maeda, K.; Ishihara, T.; Minegishi, T.; Takata, T.; Domen, K. Photocatalytic Hydrogen Evolution from Water Using Copper Gallium Sulfide under Visible-Light Irradiation. *J. Phys. Chem.* C 2010, 114, 11215–11220.
- (20) Tsuji, I.; Kato, H.; Kudo, A. Photocatalytic Hydrogen Evolution on ZnS-CuInS₂-AgInS₂ Solid Solution Photocatalysts with Wide Visible Light Absorption Bands. *Chem. Mater.* **2006**, *18*, 1969–1975.
- (21) Tsuji, I.; Shimodaira, Y.; Kato, H.; Kobayashi, H.; Kudo, A. Novel Stannite-type Complex Sulfide Photocatalysts A^I₂-Zn-A^{IV}-S₄ (A^I = Cu and Ag; A^{IV} = Sn and Ge) for Hydrogen Evolution under Visible-Light Irradiation. *Chem. Mater.* **2010**, 22, 1402–1409.
- (22) Brant, J. A.; Massi, D. M.; Holzwarth, N. A. W.; MacNeil, J. H.; Douvalis, A. P.; Bakas, T.; Martin, S. W.; Gross, M. D.; Aitken, J. A. Fast Lithium Ion Conduction in Li₂SnS₃: Synthesis, Physicochemical Characterization, and Electronic Structure. *Chem. Mater.* **2015**, 27, 189–196.
- (23) Kanno, R.; Hata, T.; Kawamoto, Y.; Irie, M. Synthesis of a new lithium ionic conductor, thio-LISICON-lithium germanium sulfide system. *Solid State Ionics* **2000**, *130*, 97–104.
- (24) Weber, D. A.; Senyshyn, A.; Weldert, K. S.; Wenzel, S.; Zhang, W.; Kaiser, R.; Berendts, S.; Janek, J.; Zeier, W. G. Structural Insights and 3D Diffusion Pathways within the Lithium Superionic Conductor Li₁₀GeP₂S₁₂. *Chem. Mater.* **2016**, 28, 5905–5915.
- (25) Liu, Z.; Fu, W.; Payzant, E. A.; Yu, X.; Wu, Z.; Dudney, N. J.; Kiggans, J.; Hong, K.; Rondinone, A. J.; Liang, C. Anomalous High Ionic Conductivity of Nanoporous β -Li₃PS₄. *J. Am. Chem. Soc.* **2013**, 135, 975–978.
- (26) Richards, W. D.; Tsujimura, T.; Miara, L. J.; Wang, Y.; Kim, J. C.; Ong, S. P.; Uechi; Suzuki, I.; Ceder, N. Design and synthesis of the superionic conductor Na₁₀SnP₂S₁₂. *Nat. Commun.* **2016**, *7*, 11009.
- (27) Wu, K.; Chu, Y.; Yang, Z. H.; Pan, S. L. A_2 SrM^{IV} S_4 (A = Li, Na; M^{IV} = Ge, Sn) concurrently exhibiting wide bandgaps and good nonlinear optical responses as new potential infrared nonlinear optical materials. *Chem. Sci.* **2019**, *10*, 3963–3968.
- (28) Guo, S. P.; Chi, Y.; Guo, G. C. Recent achievements on middle and far-infrared second-order nonlinear optical materials. *Coord. Chem. Rev.* **2017**, 335, 44–57.
- (29) Liu, B. W.; Zeng, H. Y.; Jiang, X. M.; Wang, G. E.; Li, S. F.; Xu, L.; Guo, G. C. $[A_3X][Ga_3PS_8]$ (A = K, Rb; X = Cl, Br): promising IR non-linear optical materials exhibiting concurrently strong second-harmonic generation and high laser induced damage thresholds. *Chem. Sci.* **2016**, *7*, 6273–6277.
- (30) Feng, J. H.; Hu, C. L.; Li, B. X.; Mao, J. G. LiGa₂PS₆ and LiCd₃PS₆: Molecular Designs of Two New Mid-Infrared Nonlinear Optical Materials. *Chem. Mater.* **2018**, *30*, 3901–3908.
- (31) Chen, M. C.; Wu, L. M.; Lin, H.; Zhou, L. J.; Chen, L. Disconnection Enhances the Second Harmonic Generation Response: Synthesis and Characterization of Ba₂₃Ga₈Sb₂S₃₈. *J. Am. Chem. Soc.* **2012**, *134*, 6058–6060.

- (32) Lin, X. S.; Zhang, G.; Ye, N. Growth and Characterization of BaGa₄S₇: A New Crystal for Mid-IR Nonlinear Optics. *Cryst. Growth Des.* **2009**, *9*, 1186–1189.
- (33) Brant, J. A.; Clark, D. J.; Kim, Y. S.; Jang, J. I.; Zhang, J. H.; Aitken, J. A. Li₂CdGeS₄, A Diamond-Like Semiconductor with Strong Second-Order Optical Nonlinearity in the Infrared and Exceptional Laser Damage Threshold. *Chem. Mater.* **2014**, *26*, 3045–3048.
- (34) Wu, K.; Zhang, B. B.; Yang, Z. H.; Pan, S. L. Remarkable multimember-ring configurations in a new family of Na₇M^{II}Sb₅S₁₂(M^{II}= Zn, Cd, Hg) exhibiting various three-dimensional tunnel structures. *Chem. Commun.* **2018**, *54*, 8269–8272.
- (35) Chen, R. J.; Wu, X. W.; Su, Z. Structural insights into T_2 -cluster-containing chalcogenides with vertex-, edge- and face-sharing connection modes of NaQ₆ ligands: Na₃ZnM^{III}Q₄ (M^{III} = In, Ga; Q = S, Se). *Dalton Trans.* **2018**, *47*, 15538–15544.
- (36) Klepp, K. O.; Fabian, F. Preparation and Crystal Structure of Na₃CuSnSe₄. A Novel Selenostannate(IV) with a Layered Structure. *Eur. J. Solid State Inorg. Chem.* **1997**, 34, 1155.
- (37) Teske, C. L.; Vetter, O. Ergebnisse einer Röntgenstrukturanalyse von Silber-Barium-Thiostannat(IV), Ag₂BaSnS₄. Z. Anorg. Allg. Chem. **1976**, 427, 200–204.
- (38) Teske, C. L.; Vetter, O. Praeparative und roentgenographische Untersuchung am System Cu_{2-x}Ag_xBaSnS₄. Z. Anorg. Allg. Chem. 1976, 426, 281–287.
- (39) Chen, H.; Liu, P. F.; Li, B. X.; Lin, H.; Wu, L. M.; Wu, X. T. Experimental and theoretical studies on the NLO properties of two quaternary non-centrosymmetric chalcogenides: BaAg₂GeS₄ and BaAg₂SnS₄. *Dalton Trans.* **2018**, *47*, 429–437.
- (40) Teske, C. L. Ag₂BaGeS₄/Preparation and Crystal Structure of Silver-Barium-Thiogermanate(IV). *Z. Naturforsch., B: J. Chem. Sci.* **1979**, 34b, 544–547.
- (41) Nian, L. Y.; Wu, K.; He, G. J.; Yang, Z. H.; Pan, S. L. Effect of Element Substitution on Structural Transformation and Optical Performances in $I_2BaM^{IV}Q_4$ (I=Li, Na, Cu, and Ag; $M^{IV}=Si$, Ge, and Sn; Q=S and Se). Inorg. Chem. **2018**, 57, 3434–3442.
- (42) Wang, N. New data for Ag₈SnS₆ (canfieldite) and Ag₈GeS₆ (argyrodite). Neues Jb. Miner. Monat. 1978, 269.
- (43) Ishii, M.; Onoda, M.; Shibata, K. Structure and vibrational spectra of argyrodite family compounds $Cu_8SiX_6(X = S, Se)$ and Cu_8GeS_6 . Solid State Ionics 1999, 121, 11–18.
- (44) Ji, M.; Baiyin, M. H.; Ji, S. H.; An, Y. L. Solvothermal syntheses and structures of $A_3AgSn_3Se_8$ (A = Rb, K). *Inorg. Chem. Commun.* **2007**, *10*, 555–557.
- (4S) Wu, K.; Yang, Z. H.; Pan, S. L. Na₂BaMQ₄ (M = Ge, Sn; Q = S, Se): Infrared Nonlinear Optical Materials with Excellent Performances and that Undergo Structural Transformations. *Angew. Chem., Int. Ed.* **2016**, *55*, *6713–6715*.
- (46) Kuo, S. M.; Chang, Y. M.; Chung, I.; Jang, J. I.; Her, B. H.; Yang, S. H.; Ketterson, J. B.; Kanatzidis, M. G.; Hsu, K. F. New Metal Chalcogenides $Ba_4CuGa_5Q_{12}$ (Q = S, Se) Displaying Strong Infrared Nonlinear Optical Response. *Chem. Mater.* **2013**, *25*, 2427–2433.
- (47) Mohapatra, S.; Adhikary, A.; Ghosh, K.; Choudhury, A. Magnetically Frustrated Quaternary Chalcogenides with Interpentrating Diamond Lattices. *Inorg. Chem.* **2017**, *56*, 7650–7656.
- (48) Abudurusuli, A.; Wu, K.; Rouzhahong, Y.; Yang, Z. H.; Pan, S. L. $\mathrm{Na_6Zn_3M^{III}}_2\mathrm{Q_9}$ ($\mathrm{M^{III}}=\mathrm{Ga}$, In; $\mathrm{Q}=\mathrm{S}$, Se): four new supertetrahedron-layered chalcogenides with unprecedented vertex-sharing $\mathrm{T_3}$ -clusters and desirable photoluminescence performances. *Inorg. Chem. Front.* **2018**, *5*, 1415–1422.
- (49) Axtell, E. A., III; Kanatzidis, M. G. First Examples of Gold Thiocadmates: $A_2Au_2Cd_2S_4$ (A = Rb, Cs) and $K_2Au_4CdS_4$: Bright Photoluminescence from New Alkali Metal/Gold Thiocadmates. *Chem. Eur. J.* **1998**, *4*, 2435–2441.
- (50) Axtell, E. A., III; Liao, J. H.; Pikramenou, Z.; Kanatzidis, M. G. Dimensional reduction in II-VI materials: $A_2Cd_3Q_4$ (A = K, Q = S, Se, Te; A = Rb, Q = S, Se), novel ternary low-dimensional cadmium chalcogenides produced by incorporation of A_2Q in CdQ. Chem. Eur. J. 1996, 2, 656–666.

- (51) Zhen, N.; Wu, K.; Wang, Y.; Li, Q.; Gao, W. H.; Hou, D. W.; Yang, Z. H.; Jiang, H. D.; Dong, Y. J.; Pan, S. L. BaCdSnS₄ and Ba₃CdSn₂S₈: syntheses, structures, and non-linear optical and photoluminescence properties. *Dalton Trans.* **2016**, 45, 10681–10688.
- (52) Godby, R. W.; Schlüter, M.; Sham, L. J. Self-energy operators and exchange-correlation potentials in semiconductors. *Phys. Rev. B: Condens. Matter Mater. Phys.* **1988**, *37*, 10159–10175.
- (53) Shi, Y. F.; Chen, Y. K.; Chen, M. C.; Wu, L. M.; Lin, H.; Zhou, L. J.; Chen, L. Strongest Second Harmonic Generation in the Polar R₃MTQ₇ Family: Atomic Distribution Induced Nonlinear Optical Cooperation. *Chem. Mater.* **2015**, *27*, 1876–1884.